



Galvanomagnetic properties of dislocations in GaAs

D. Ferré, J.L. Farvacque

► To cite this version:

D. Ferré, J.L. Farvacque. Galvanomagnetic properties of dislocations in GaAs. *Revue de Physique Appliquée*, 1990, 25 (4), pp.323-332. 10.1051/rphysap:01990002504032300 . jpa-00246190

HAL Id: jpa-00246190

<https://hal.science/jpa-00246190>

Submitted on 4 Feb 2008

HAL is a multi-disciplinary open access archive for the deposit and dissemination of scientific research documents, whether they are published or not. The documents may come from teaching and research institutions in France or abroad, or from public or private research centers.

L'archive ouverte pluridisciplinaire **HAL**, est destinée au dépôt et à la diffusion de documents scientifiques de niveau recherche, publiés ou non, émanant des établissements d'enseignement et de recherche français ou étrangers, des laboratoires publics ou privés.

Classification

Physics Abstracts

71.55Eq — 72.10Fk — 72.20M

Galvanomagnetic properties of dislocations in GaAs

D. Ferré and J. L. Farvacque

Université des Sciences et Techniques de Lille Flandres Artois, 59655 Villeneuve d'Ascq Cedex, France

(Reçu le 19 septembre, révisé le 7 décembre 1989, accepté le 15 décembre 1989)

Résumé. — Des mesures de conductivité et d'effet Hall effectuées sur des échantillons de GaAs déformés plastiquement ont été analysées au moyen de simulations théoriques de l'effet Hall et de la résistivité induite par les mécanismes de diffusion associés aux dislocations. Cette analyse confirme que les dislocations de glissement induisent l'existence d'une bande unidimensionnelle à caractère amphotère et située très légèrement au-dessus de la bande de valence. Le mécanisme de diffusion le plus efficace semble être associé au potentiel de déformation qui est renforcé par le potentiel coulombien dans le cas où les dislocations sont suffisamment chargées (cas des échantillons de type n).

Abstract. — Galvanomagnetic measurements on plastically deformed GaAs have been compared with theoretical calculations of the Hall effect and of the induced resistivity associated with dislocation scattering mechanisms. This analysis allows us to confirm that dislocations are responsible for the existence of an amphoteric one-dimensional energy band located very near the top of the valence band. It also points out that scattering mechanisms acting on the free carrier mobility are mainly connected with the deformation potential reinforced by the Coulomb potential when dislocations are sufficiently charged (case of n type materials).

1. Introduction.

Since the pioneer works on covalent semiconductors by Read and Morin [1-3], it has been well known that dislocations can modify drastically the galvanomagnetic properties of any semiconductor. This explains why some performances of microdevices are frequently limited by the presence of isolated dislocations within their active area. In such devices, limited performances or ageing phenomena originates, most of the time, from as-grown dislocations and their interaction with points defects. These last effects come either from mechanical mechanisms or, more directly, from the intrinsic properties of the dislocations themselves (dangling bond or not, appearance of internal electric field connected with the dislocation charge a.s.o...). So, it is of prime importance to determine what the electronic properties of dislocations are, even if these ones have been introduced by plastic deformation and do not directly correspond to as-grown defects.

In view to answering to the two main questions :

— do dislocations introduce deep states in GaAs ?

— what are the most efficient scattering mechanisms associated with dislocations ?

We have performed conductivity and Hall effect measurements on plastically deformed GaAs. To our knowledge, the previous papers concerning galvanomagnetic measurements in deformed GaAs, [4-7] only give a qualitative explanation of the free carrier mobility. On the contrary, our approach allows to determine quantitatively the order of magnitude of the induced resistivity. The Hall effect has been simulated by applying a modified Read-like calculation for the dislocation statistics. The experimental resistivity have been compared with theoretical calculations of the induced resistivity obtained from the « energy loss method » [8-10].

This comparison firstly allows us to confirm that dislocations introduce a one-dimensional energy band within the band gap, located near the valence band in good agreement with photoluminescence and optical absorption measurements [11-13]. Secondly, it indicates that, in the case of n type materials, dislocations act on the free carrier mobility through two different mechanisms : 1) the Coulomb potential associated with the carriers trapped at the

dislocation band and 2) the deformation potential calculated with the help of its theoretical expression deduced in [14]. In the case of p type materials for which dislocations are only weakly charged, scattering effects can only be caused by the deformation potential. Although the theoretical analysis has been made with concepts which are already published, the process is not obvious and we shall present it, therefore, in the second part of this paper in order to point out where the most delicate approximations are. The third part will be devoted to the experimental results and, finally, to their interpretation.

2. The general frame of theoretical simulations.

The theoretical model used to perform simulation of the Hall effect remains very close to Read's model which has been established for the particular case of covalent semiconductors. It has been adapted in order to account for the specificities of III-V compounds (more particularly, the crystal ionicity must be taken into account in the definition of the dislocation neutral state) and to introduce new effects such as the non rigid shift of the dislocation band *versus* the crystal band, when free carriers are trapped at the dislocation.

These points are explicitly precised in the following.

2.1 THE OCCUPATION STATISTICS.

2.1.1 Read's model and the rigid shift. — Contrary to points defects, core atoms along the dislocation line must be considered as interactive traps, because they are close to one another (distant one atomic spacing). Consequently, 1) the electronic states associated with core atoms form a one-dimensional energy band, 2) the electrostatic interaction between trapped carriers is very strong ; this is responsible for a self regulation of the electron density n_t trapped at the dislocation band. It is easy to show that n_t verifies :

$$n_t = \frac{2D}{b} \left[\frac{1}{1 + \exp\left(\frac{E_d^* - F}{kT}\right)} - \chi \right] \quad (1)$$

where n_t represents the number of trapped electrons per unit volume ; it can be either positive when the dislocation has trapped electrons or negative when the dislocation has lost electrons ; D is the total length of dislocation line per unit volume ; b is the dislocation Burgers vector ; χ is the occupation rate of the neutral dislocation ; F is the Fermi level ; E_d^* is an « effective » level whose position, within the energy band gap, is dependent on the total number n_t of electrons trapped at the dislocation line.

$$E_d^* = E_d^0 + \alpha n_t. \quad (2)$$

In Read's theory [2, 3], the term αn_t arises only from the electrostatic interaction of the trapped carriers. At the first order in perturbation, it is then responsible of a rigid shift of any crystal state located at the dislocation core. This term corresponds to the derivative *versus* n_t of the total free energy increase of the crystal. The latter quantity depends itself on the crystal screening properties. Screening effects result simultaneously i) from an upper ionisation of the donors and acceptors when they are not totally thermally ionized (for instance, this may correspond to the case of shallow impurities at low temperature or to the case of deep levels), ii) from the dielectric properties of the free carriers themselves. There are currently, two ways of evaluating such screening effects but which correspond in fact to two different physical situations : either the screened potential is large, indicating that dislocation lines are mainly surrounded by a depleted region, or this potential remains weak in most regions surrounding the dislocation and it essentially leads to some modification of the free carrier distribution around the dislocation lines. The first situation has been chosen by Read who then used the depleted region approximation, in a way similar to the one currently used for evaluating the electric field at a Schottky diode. The screening effects corresponding to the second situation, but limited to the case of one class of free carrier, was proposed and calculated latter on by Labusch and Schröter [15]. Their results could be recovered in [16] by making use of the free carrier dielectric function evaluated in the Debye-Hückel approximation. Moreover, this procedure allowed us to extend the calculation to the case of more complex situations where ionisable impurities and more than one class of free carrier are simultaneously present [10]. This requires to replace the standard Debye-Hückel screening length by a generalised screening length λ_G defined as follows :

$$\lambda_G = 1/k_G$$

with

$$k_G^2 = \frac{e^2}{\epsilon_0 \epsilon_l kT} \left[n + p + \sum_i \frac{N_{Di}^+ (N_{Di} - N_{Di}^+)}{N_{Di}} + \sum_i \frac{N_{Ai}^- (N_{Ai} - N_{Ai}^-)}{N_{Ai}} \right]. \quad (3)$$

Thus, the rigid shift is given by :

$$\alpha n_t = \frac{n_t e^2}{2 \pi \epsilon_0 \epsilon_l D} \left[\text{Log} \left(\frac{\lambda_G}{b} - 1/2 \right) \right] \quad (4)$$

b is the dislocation Burgers vector.

This procedure for evaluating the dislocation statistics has been chosen in the present paper. Let us, nevertheless, remark that this kind of screening calculation leads to rigid shift values which, most of

the time, are large at the dislocation line when compared to kT . Thus it does not strictly correspond to the validity range of the Debye-Hückel approximation. The latter fact results in a slight overestimate of the density of carriers trapped at the dislocation line. An exact selfconsistent calculation of the screening effects by numerically solving Poisson's equation allows to specify the validity range of the Debye-Hückel approximation [17].

2.1.2 The non rigid shift. — For covalent semiconductors as well as for III-V compounds (for edge type dislocations at least), energy states — when they exist — fundamentally originate from « dangling bonds » which are left uncoupled by the modification of the number of first neighbours around each core atom. This fact remains true even when dislocation cores are reconstructed. These hybrid orbitals are built up with s and p atomic orbitals whose eigen energies depend on the total atomic electrical charge. Thus, owing to this intra atomic interaction, which has nothing to do with the electrostatic interaction between trapped carriers, the relative position of the sp_3 orbitals *versus* the crystal bands will be dependent on the mean charge trapped at each dislocation site. This « non rigid » shift proposed by Lannoo *et al.* [18] can be roughly evaluated by the following expression :

$$\Delta E_d = \frac{J n_t}{\epsilon_l D} \quad (5)$$

n_t/D is the number of excess electron per site in the dislocation core, ϵ_l the dielectric constant. J/ϵ_l characterise the intra atomic interaction ; its order of magnitude corresponds to the change of the sp_3 energy at the first ionisation, screened by the static dielectric response of the material. This non rigid shift must then be added to the rigid shift for final evaluation of the dislocation occupation statistics.

2.1.3 Delocalisation effects. — Most of the time, the calculation of the electrostatic interaction between trapped carriers is made by considering that carriers are strictly localized at the dislocation line. One can nevertheless consider the possibility of a noticeable radial extension of the dislocation states which will lead to a decrease of the interaction energy [19]. This effect can be linearized for small delocalisations and will generally lead to numerical effects which are equivalent either to a slight increase of the dislocation density or, even, to a modification of the term J in the non rigid shift expression. This delocalisation effect cannot be, in practice, distinguished from these other effects and will not be considered in the following.

2.1.4 Occupation rate of the neutral dislocation. — Let us consider a simple model where dislocation energy states are coming from an array of dangling bonds and give rise to an energy band. In

covalent semiconductors, such a band is obviously neutral when the dislocation band is half filled. The situation is no longer the same for ionic materials. Let us define the dislocation neutrality as corresponding to a charge state which leaves the energy bands at the surrounding of the dislocation core flat. From a metallurgical point of view, creating a 60° dislocation in III-V materials can be seen as if we were removing half an atomic plane ending at a row of identical atoms. In ionic materials, this will give rise to an infinite increase of the Madelung energy, though the crystal remains electrically neutral. Thus, a charge transfert along the dislocation line must be necessary to balance this infinite increase. Owing to lattice distortions around the dislocation line, the actual variation of the Madelung term and the actual charge borne by the « neutral » dislocation is not easily calculated. Nonetheless, it may be roughly estimated by assuming that the charge state at the dislocation core results from a charge transfert equivalent to that at the origin of the charge on polar surfaces. Thus, following [20], χ will be either equal to $3/8$ or $5/8$ depending on the nature of core atoms.

2.2 SCATTERING MECHANISMS. — Before describing the different scattering mechanisms which can be associated with dislocations, let us recall that mobility calculations have been made with the help of the « energy loss » method [8-10]. This method is based on the equivalency between Joule's heat and the energy lost by the reciprocal motion of the scattering centers seen in a reference frame where the free carriers are at rest. This energy loss corresponds then to the work done by the scattering charge motion through the induced electrical field coming from the dielectric response of the free carriers. These induced fields are calculated with the help of Lindhard's dielectric function, evaluated in Debye-Hückel's approximation. This method only needs the knowledge of the Fourier transform of the bare scattering potential.

The various scattering mechanisms associated with dislocations are now well known and can be connected either with core effects or with the long range strain fields of the dislocations.

2.2.1 The core effects. — This scattering mechanism can only be associated with dislocations as long as they introduce one-dimensional energy bands in the crystal band gap. In such a case, some Coulomb potential V_C comes from the presence of free carriers trapped along the dislocation lines. Let us denote by f the linear density of charge along the dislocation. The Fourier transform calculation of the Coulomb potential of this bared charge line is then straightforward and is given by :

$$V_C(\mathbf{q}) = \frac{f 2 \pi \delta(q_z)}{\epsilon_0 q^2} \quad (6)$$

2.2.2 Potentials associated with the stress field. — A dislocation creates a inhomogeneous stress field which is responsible for a displacement of the ions from their ideal crystallographic sites and also for a deformation of each ion. The inhomogeneous displacement gives rise to the so called « deformation potential » and the ion deformation may result, in non centrosymmetric crystals, to piezoelectrical effects.

2.2.2.1 The piezoelectrical scattering. — The possibility of a piezoelectrical scattering by dislocations has been simultaneously proposed by Merten [21] and by Levinson [22]. In principle, the piezoelectrical field must be calculated by solving the selfconsistent set of Voigt's equations :

$$\begin{aligned}\sigma &= c : \epsilon + e \cdot E \\ D &= e : \epsilon + \chi \cdot E\end{aligned}\quad (7)$$

where σ is the stress tensor, ϵ the strain tensor, χ the dielectric tensor ; e is the piezoelectric tensor and E and D are the electric and displacement fields. Nonetheless, it has been shown in [23, 24] that the deformation field could be in practice evaluated by neglecting coupling effects, i.e. by neglecting the electrical field in equation (a). Furthermore, it has been shown in [25] that for III-V compounds, at least, the elastic anisotropy could also be neglected. So, in practice, the piezoelectrical bare potential is obtained i) by solving $\sigma = c : \epsilon$ in the elastic approximation and ii) by suppressing from (b) the dielectric response $\chi \cdot E$. This gives for its Fourier transform :

$$V_{\text{piezo}}(\mathbf{q}) = \frac{-iq(e : \epsilon(\mathbf{q}))}{\epsilon_0 q^2} \quad (8)$$

where $\epsilon(\mathbf{q})$ turns out to be an imaginary function.

Following [25], no effect is associated with a screw dislocation and the edge component only gives a piezoelectrical contribution to the scattering. The Fourier transform of the piezoelectrical scattering potential is given by :

$$V_{\text{piezo}}(\mathbf{q}) = \frac{2 \pi b e_{14}}{\epsilon_0 \epsilon_l(3)^{1/2}} F(\theta) \frac{\delta(q_z)}{q^2} \quad (9)$$

e_{14} is the element of the piezo electrical tensor e , b is the edge component of the Burgers vector. $F(\theta)$ describes the angular dependence of the potential in a plane perpendicular to the dislocation line ; its expression is given explicitly in [25].

2.2.2.2 The deformation potential. — The deformation potential associated with a dislocation has been introduced for the first time by Dexter and Seitz [26] for evaluating residual resistivity of « cold-worked » metals. The expression used for describing this potential corresponds to the one which has been

used for calculating acoustical phonon scattering. It corresponds in fact to an extension of the piezo resistivity tensor to the case of inhomogeneous strain fields : his potential is given by [27] :

$$V_{\text{dp}}(\mathbf{r}) = E_1 \text{Tr}(\epsilon(\mathbf{r})). \quad (10)$$

This form of deformation potential leads, when introduced in the « energy loss » formula to negligible resistivity effects [28]. This numerical result may be explained by remembering that the deformation potential constant E_1 directly comes from experimental data so that formula (10) would rather correspond to an already screened potential, which cannot therefore be used in the energy loss calculation.

In order to obtain an evaluation of the bare deformation potential, let us notice that homogeneous stresses do not obviously introduce any special scattering effect since they simply induce an homogeneous variation of the crystal parameters. It can only induce some modifications of the energy bands. The physical phenomena resulting from such a band structure deformation may only correspond to some modification of the free carrier density in some given conductivity valleys but not specially to scattering phenomena. So, it would be surprising that the deformation potential constants measured under homogeneous stresses should successfully be used in the case of inhomogeneous deformation. However, when a crystal is inhomogeneously deformed, it is clear that the electron Bloch functions specially adapted to the crystal periodicity will no longer be good solutions in the stressed region and will be scattered. Following [14] we may define a bare scattering potential corresponding to the difference between pseudo-potentials associated with ions placed at the ideal crystal sites (undeformed lattice) and those associated with ions displaced from their equilibrium position by the strain field :

$$\begin{aligned}V_{\text{dp}}(\mathbf{r}) &= \sum_j V_{\text{ion}}(\mathbf{r} - \mathbf{R}_j - \mathbf{u}(\mathbf{R}_j)) - V_{\text{ion}}(\mathbf{r} - \mathbf{R}_j) \\ &\approx \sum_j \text{grad}(V_{\text{ion}}(\mathbf{r} + \mathbf{R}_j)) \cdot \mathbf{u}(\mathbf{R}_j).\end{aligned}\quad (11)$$

The Fourier transform of the previous expression is directly given by :

$$V_{\text{dp}}(\mathbf{q}) = N/8 \pi^3 \cdot V_{\text{ion}}(\mathbf{q}) \sum_{\mathbf{G}} i \mathbf{q} \cdot \mathbf{u}(\mathbf{q} + \mathbf{G}). \quad (12)$$

Assuming that the ion pseudo potentials vary weakly in space, umklapp terms may be neglected ; the term $\mathbf{q} \cdot \mathbf{u}$ is then equal to $\text{Tr}(\epsilon)$; so that :

$$V_{\text{dp}}(\mathbf{q}) = N/8 \pi^3 \cdot V_{\text{ion}}(\mathbf{q}) \text{Tr}(\epsilon(\mathbf{q})). \quad (13)$$

This expression cannot be directly compared with the Bardeen and Shockley formula since it corre-

sponds to the convolution product between the ion pseudo potential and the strain field. In any case, it cannot be reduced to the simple product of a given constant with $\text{Tr}(\epsilon)$. The latter expression is specially well adapted to the case of the « energy loss » method and leads to induced resistivities much more important than those obtained with the Bardeen and Shockley's formula.

2.2.3 Efficiency of the different scattering mechanisms. — The energy loss method needs to know the square modulus of the total scattering potential. In the case of dislocations, this potential is the sum of three terms : electrostatic, piezoelectric and deformation potentials. It results from this that the induced free carriers mobility depends not only on each scattering mechanisms but also on their coupling. Therefore, the total scattering effect of dislocations does not only result from additive contributions, which would lead to the use of Matthiessen's rule.

Let us however remark that, in Fourier space, electrostatic and piezoelectric potentials contributions are real functions while the deformation potential contribution is an imaginary one. Thus :

$$|V_{\text{Total}}(\mathbf{q})|^2 = |V_c(\mathbf{q}) + V_{\text{piezo}}(\mathbf{q})|^2 + |V_{\text{dp}}(\mathbf{q})|^2. \quad (14)$$

Then, it becomes possible to study separately the deformation potential contribution to the mobility of the free carriers. The results of a numerical calculation, reported in figure 1, show that this contri-

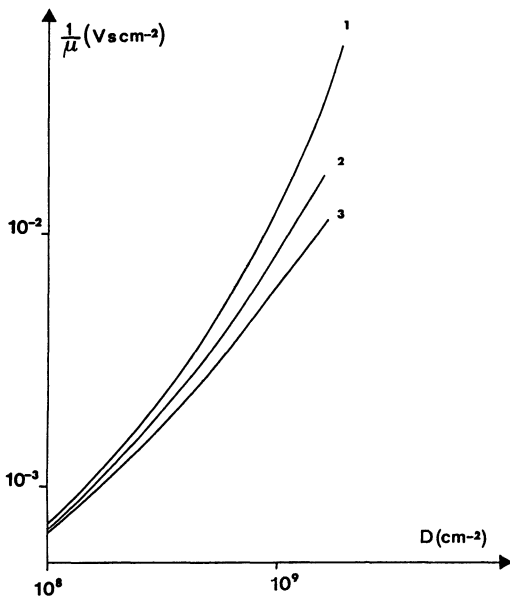


Fig. 1. — Deformation potential contribution to the mobility of free carriers in *n*-GaAs (as calculated in [14]). $T = 77$ K. The energy level associated with neutral dislocation is located (1) $E_d^0 = 130$ meV, (2) $E_d^0 = 650$ meV, (3) $E_d^0 = 1\,040$ meV from the top of the valence band.

bution is very strong but quite insensitive to the position E_d^0 of the energy level associated with the neutral dislocation.

The reduction of the free carriers mobility induced by the combined effect of electrostatic and piezoelectrical potentials is analysed in figure 2. The main contribution of these two potentials is the electrostatic one. Owing to the fact that it depends on the trapped charge along the line, it is very sensitive to the energy level position E_d^0 .

In conclusion, deformation potential is only effective scattering mechanism when dislocations are weakly charged. In the opposite case, deformation potential and electrostatic potential become competitive. Piezoelectrical potential contribution is never the major one. Thus, we only retain in the following analysis, the electrostatic and the deformation potentials for which Matthiessen's rule can be applied.

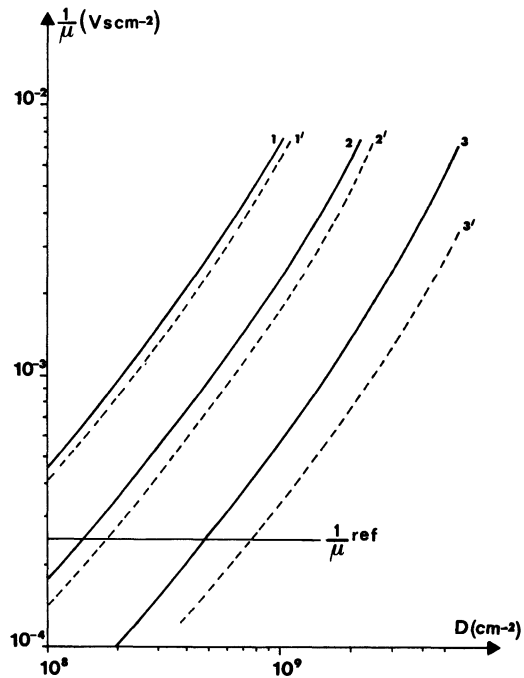


Fig. 2. — Contribution of the piezoelectrical and electrostatic potentials to the mobility of free carriers in *n*-GaAs. $T = 77$ K. (—) Effect of piezoelectrical and electrostatic potentials. (-----) Effect of electrostatic potential alone. The energy level associated with neutral dislocation is located at (1) $E_d^0 = 130$ meV, (2) $E_d^0 = 650$ meV, $E_d^0 = 1\,040$ meV from the top of the valence band. The electronic mobility of the reference material is also shown for comparison.

3. Experimental conditions and results.

In order to compare trapping and scattering effects by dislocations in *n* and *p* type materials, it is obviously necessary to deal with identical dislocation

substructures. In the case of GaAs, it is well known that dislocation velocity is dependent on the doping type and concentration. For weakly doped materials however, the dislocation velocity is roughly the same for n and p type materials [29]. Such materials with $n \approx p \approx 10^{16} \text{ cm}^{-3}$ have been used in the present work in order to obtain identical dislocation substructures at equivalent deformation conditions.

Uniaxial compression tests have been performed in air at $T = 450^\circ \text{C}$ in the classical $\langle 123 \rangle$ orientation up to various deformation levels (typically $1\% < \varepsilon < 7\%$). The strain rate was about $3 \times 10^{-5} \text{ s}^{-1}$. After deformation, specimens were cooled in the furnace at a low rate without applying the load. Under these experimental conditions, dislocation substructures left within the samples are mainly constituted of segments close to pure edge orientation contrary to the case of lower deformation temperature ($T < 300^\circ \text{C}$) for which the Peierls friction favours the screw orientation [30]. Numerous debris and dipoles are also observed, probably due to dislocation intersections. These intersections may, in turn, result in a large density of point defects.

Samples used for electrical measurements possess the same orientation than those used for plastic deformation i.e. the electrical current is parallel to the $\langle 123 \rangle$ direction. Hall effect and conductivity have been measured between 77 K and 300 K. Satisfactory ohmic contacts were achieved by alloying tin at $T \approx 480^\circ \text{C}$ in an atmosphere of H_2 and NH_4Cl . This method is well adapted to the geometry of the measured specimens and gives contacts which never showed significant differences compared to the standard vacuum deposited Au-Ge-Ni contacts. The possible contamination during the deformation test has been checked by comparing reference samples with undeformed samples which have been submitted to the same thermal treatment as the deformed ones. Hall effect measurements were carried out using the standard dc technique, at sufficiently low magnetic field ($B < 5\,000 \text{ Gauss}$) to ensure that R_H does not depend on B .

Figures 3 and 4 represent, respectively for n and p type materials, the Hall constant *versus* temperature at various deformation levels. Generally speaking, these results show that plastic deformation is responsible for a noticeable decrease in the free carrier density for n as well as p type samples. It indicates that defects introduced by plastic deformation possess an overall amphoteric character. One notices that the evolution of the free carrier trapping efficiency parallels that of the deformation level and is of the same order of magnitude in n and p type materials for an equal amount of deformation. Conductivity measurements show that the free carrier mobility, reported in figures 5 and 6 is strongly reduced in both n and p type materials. For a 6%

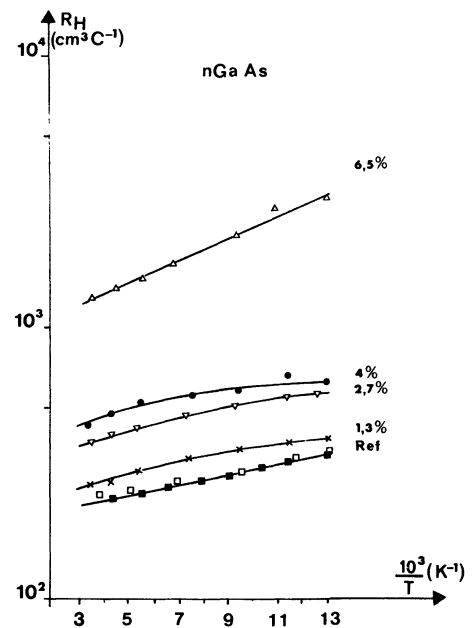


Fig. 3. — Plot of the Hall constant *versus* reciprocal temperature in deformed n -GaAs, for various strain levels. (\square , \blacksquare) reference, (\times) 1.3 %, (∇) 2.7 %, (\bullet) 4 %, (Δ) 6.5 %.

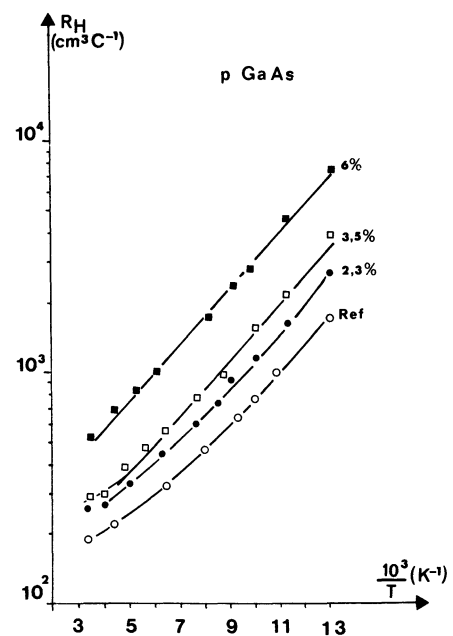


Fig. 4. — Plot of the Hall constant *versus* reciprocal temperature in deformed p -GaAs for various strain levels. (\circ) reference, (\bullet) 2.3 %, (\square) 3.5 %, (\blacksquare) 6 %.

deformation level, the induced mobility evaluated according Matthiessen's rule is about $10 \text{ cm}^2 \text{ V}^{-1} \text{ s}^{-1}$ at 77 K in n type material.

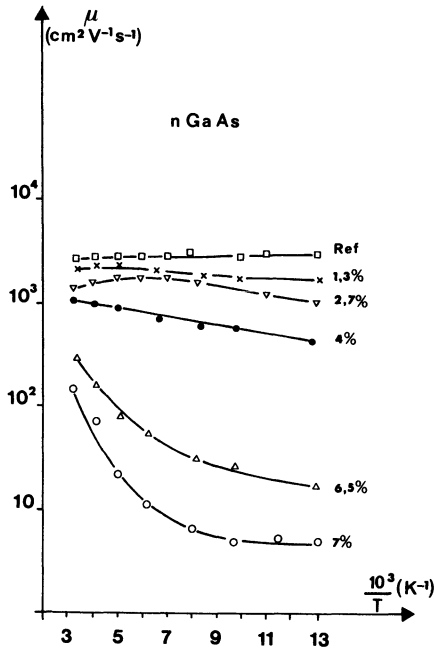


Fig. 5. — Variation of the Hall mobility as a function of reciprocal temperature in deformed *n*-GaAs for various strain levels. (□) reference, (×) 1.3 %, (▽) 2.7 %, (●) 4 %, (△) 6.5 %, (○) 7 %.

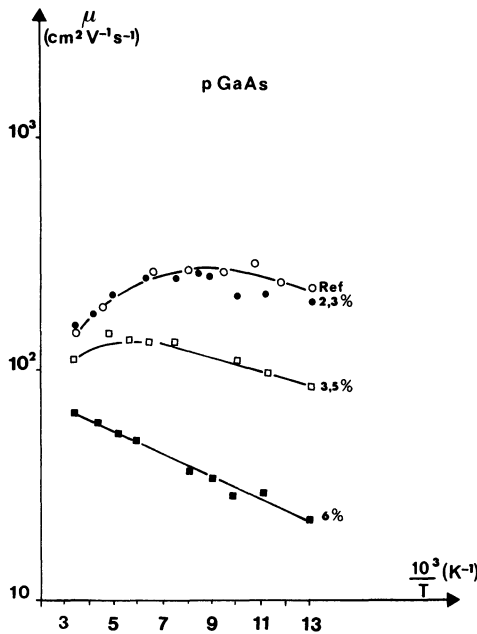


Fig. 6. — Variation of the Hall mobility as a function of reciprocal temperature in deformed *p*-GaAs for various strain levels ; (○) reference, (●) 2.3 %, (□) 3.5 %, (■) 6 %.

4. Discussion.

As soon as the various types of defects contained in a reference material are well characterized, its electrical neutrality can be used to localize the Fermi level.

If one postulates that defects (or impurities) initially present in the material remain unchanged after deformation, the electrical neutrality equation is given by :

$$p - n + \sum_i N_{Di}^+ - \sum_i N_{Ai}^- + [\text{Def}] = 0 \quad (15)$$

where the charge borne by plastic deformation induced defects is represented by the quantity between brackets. Moreover, measurements of the free carrier density can be used to determine the position of the Fermi level. Therefore, the quantity $[\text{Def}]$ may be deduced for each deformed sample.

Plastic deformation may be responsible for both the appearance of extrinsic levels associated with dislocations and point defects resulting from either dislocation glide or intersections. In such a case, the quantity $[\text{Def}]$ is equal to the total charge n_t trapped at the dislocation plus the density D_p of ionized deep traps. Using the dislocation occupation statistics, described in the first part of the paper, it is therefore possible to calculate, for any arbitrary position of the dislocation level E_d^0 , the excess of charge n_t/Db . From this previous calculation, the point defect density can be evaluated as follows : point defects are assumed to correspond to deep states whose ionization is temperature independent. We have thus :

$$\frac{n_t(T_1)}{n_t(T_2)} = \frac{[\text{Def}(T_1)] - D_p}{[\text{Def}(T_2)] - D_p} \quad (16)$$

the ratio $n_t(T_1)/n_t(T_2)$ is, obviously independent of the active dislocation density. The quantity D_p and the electrically active dislocation density can then be determined as a function of the dislocation level position. E_d^0 is chosen in order to yield the best fit of the Hall constant vs. T curve.

Applying this method shows that a continuous choice of the triplet (E_d^0 , N_D , D_p) values can be made, each of them leading to a sufficiently good agreement with the experimental Hall measurements.

Therefore, for any arbitrary value of the dislocation level E_d^0 it is always possible to determine the densities of both the ionized point defects and the electrically active dislocations which are coherent with the Hall constant measurements.

The latter analysis shows that it seems impossible to determine simultaneously the energy position of the dislocation level, the dislocation density and the point defect density from the knowledge of the Hall effect alone. These measurements must necessarily be completed by other experiments like, for instance, an estimate of the point defect density (as it has been done in [4]) or an estimate of the electrically active dislocation density as it has been done in the following.

However, there is no classical way of determining experimentally (by etch pit counting or TEM evaluation for instance) the electrically active dislocation density with a sufficiently great accuracy for the present purpose. Thus, the method which is proposed here consists in analysing the mobility curves and in choosing the final (D, E_d^0) couple value leading to the best theoretical agreement.

4.1 POINT DEFECT SCATTERING. — In order to evaluate the role played by point defects on the free carrier mobility, let us notice that the maximum point defect density corresponds to the case where no extrinsic levels would be associated with dislocations. In such a case, their density is equal to the experimental variation of the free carrier density. The induced inverse mobility associated with such an over-estimate of ionized point defects is always very low ($\approx 10^{-4} \text{ V s cm}^{-2}$). Comparison with the experimental inverse mobility obtained by applying Matthiessen's rule clearly shows that the maximum point defect density cannot be associated with the experimentally observed free carrier induced resistivity. Therefore, the strong resistivity effect may only come from dislocation scattering mechanisms.

4.2 DISLOCATION SCATTERING MECHANISMS.

4.2.1 Case of *n* type materials. — The numerical calculations of dislocation scattering effect were done for different triplets (E_d^0, N_D, D_p) which all agree with Hall constant measurements. They show that the only way to get the right order of magnitude of the mobility decrease is to evoke simultaneously 1) the deformation potential as calculated in [14] and 2) the core effect associated with a strong dislocation charge. The best agreement, for a sample deformed by an amount of 6 %, corresponds to an active dislocation density of the order of $1.2 \times 10^9 \text{ cm}^{-2}$ and to a dislocation level close to the top of the valence band (see Fig. 7). As it has been noted previously, the point defect scattering, the piezo-electrical potential as well as the Bardeen and Shockley expression of the deformation potential lead to negligible contributions.

4.2.2 Case of *p* type materials. — If the dislocation level is located close to the valence band, in *p* type material, dislocations are weakly charged and the reduction of the free carrier density results from trapping at point defects. The only effective scattering mechanism is then associated with deformation potential. A sufficiently good agreement between numerical and experimental values of the mobility was obtained if the dislocation density is taken of the same order of magnitude as in *n* type material for comparable deformation (see Fig. 8). Again, the experimental results in *p* type material are consistent with locating the dislocation level very close to the top of the valence band.

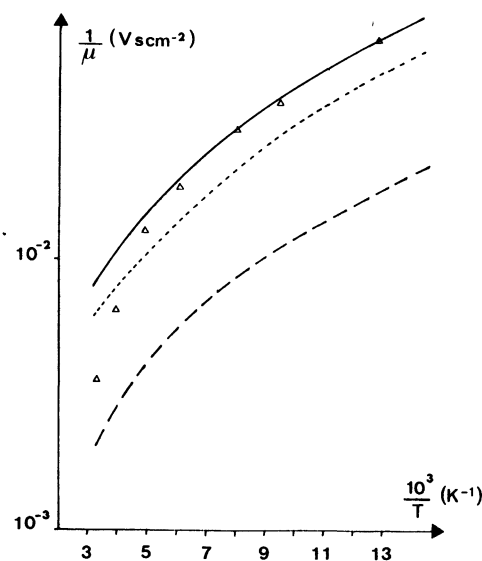


Fig. 7. — Experimental and calculated inverse mobility in *n* type GaAs (Δ) experimental points for a 6.5 % deformed sample. (—) Electrostatic potential contribution. (-----) Deformation potential contribution. (—) Total effect of electrostatic and deformation potentials. Parameters of the numerical analysis are $D = 1.2 \times 10^9 \text{ cm}^{-2}$, $E_d^0 = 130 \text{ meV}$.

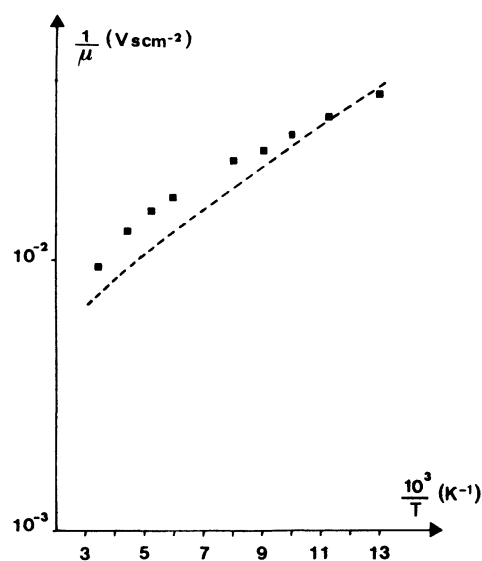


Fig. 8. — Experimental and calculated inverse mobility in *p* type GaAs. (\blacksquare) Experimental points for a 6 % deformed sample. (-----) Deformation potential contribution. Parameters of the numerical analysis are $D = 1.2 \times 10^9 \text{ cm}^{-2}$, $E_d^0 = 130 \text{ meV}$.

4.3 COMPARISON WITH ALREADY PUBLISHED EXPERIMENTAL RESULTS AND ANALYSIS. — The present analysis shows that our experimental results can be explained by the presence of, at least, one dislocation energy band just above the valence band and the presence of point defect-like energy levels.

It has been shown, however, in [31] that, in the extrinsic temperature range of GaAs, a dislocation band lying deep in the band gap would have a statistical occupation quite temperature independent. Such a band cannot be, therefore, easily distinguished from point defect levels. Thus, galvanomagnetic measurements are then unable to clearly evidence such deep dislocation bands. Since our results are consistent with deep states, we do not exclude the possibility of other dislocation bands located deeper in the band gap than the one evidenced in the present study. So, our conclusions are not inconsistent with those deduced from optical [32] and D.L.T.S. [6] measurements. Discrepancies arise between our results and others, already published [4], locating the dislocation band at 0.4 eV above the valence band. We could have found an identical value by choosing an appropriate dislocation density but the mobility calculation, with such an energy position would have lead too weak a mobility effect in *n* type materials and, on the contrary, to too large a mobility effect in *p* type materials. Moreover, contrary to the present study, results of [5] have not evidenced any trapping effect in the case of *p* type materials. Let us notice however that the deformation procedure is strongly different of our (sample orientation and deformation rate) so that any direct comparison is very difficult to do. Further studies are obviously needed to clarify this point.

5. Conclusion.

The analysis of the present galvanomagnetic measurements confirms that dislocations introduced by high temperature plastic deformation are responsible for the existence of extrinsic levels. The proposed theoretical model enables to account for the observed behaviour with a single, one dimensional, amphoteric energy band located close to the top of the valence band. The present data also indicate that a large amount of point defects is simultaneously introduced in the crystal by plastic deformation and may correspond to acceptor as well as donor states. The free carrier mobility is strongly affected by plastic deformation. However, the order of magnitude of the induced resistivity rules out any preeminent role played by point defects. The experimental observed resistivity can be predicted by means of the deformation potential as long as it is relevant to the formula derived in [14]. Since no other scattering mechanism found in the literature is able to give the right order of magnitude, the present work tend to validate the proposed theoretical expression of the deformation potential. Depending on the Fermi level position, the charge borne at the dislocation line is also responsible for a noticeable scattering effect. It adds to the deformation potential effect in the case of *n* type materials where dislocations are strongly charged, but does not play any significant role in the case of *p* type materials where dislocations are only weakly charged.

References

- [1] PEARSON G. L., READ W. T., MORIN F. J., *Phys. Rev.* **93** (1954) 666.
- [2] READ W. T., *Philos. Mag.* **45** (1954) 775 and 1119.
- [3] READ W. T., *Philos. Mag.* **46** (1955) 111.
- [4] GERTHSEN D., *Phys. Status Solidi (a)* **110** (1986) 527.
- [5] SKOWRONSKI M., LAGOWSKI J., MILSTEIN M., KANG C. H., DABKOWSKI F. P., HENNEL H., GATOS H. C., *J. Appl. Phys.* **62** (1987) 3791.
- [6] WOSINSKI T., Intern. Conf. on the Science and Technology of defect control in Semiconductors (Yokohama) 1989.
- [7] SUEZAWA M., SUMINO K., *Jpn J. Appl. Phys.* **25** (1986) 533.
- [8] GERLACH E., *Phys. Status Solidi (b)* **61** (1974) K97.
- [9] GERLACH E., GROSSE P., *Festkörperprobleme XVII* (1977) p. 157.
- [10] FARVACQUE J. L., VIGNAUD D., *Phys. Rev. B* **31** (1985) 1041.
- [11] FARVACQUE J. L., VIGNAUD D., Proc. 13th Int. Conf. on defects in semiconductors. Ed. L. C. Kimerling, J. M. Parsey, (Metallurgical society publisher) 1985, p. 373.
- [12] DEPRAETERE E., VIGNAUD D., FARVACQUE J. L., *Solid State Commun.* **64** (1987) 1465.
- [13] VIGNAUD D., FARVACQUE J. L., *J. Appl. Phys.* **65** (1987) 1261.
- [14] FARVACQUE J. L., LENGART P., *Phys. Status Solidi* **80** (1977) 361 and 433.
- [15] SCHROTER W., LABUSCH R., *Phys. Status Solidi* **36** (1969) 539.
- [16] MASUT R., PENCHINA C. M., FARVACQUE J. L., *J. Appl. Phys.* **53** (1982) 4864.
- [17] FERRE D., DIALLO A., FARVACQUE J. L., *Revue Phys. Appl.* **25** (1990).
- [18] VETH L., LANNOO M., *Philos. Mag. B* **50** (1984) 93.
- [19] FARVACQUE J. L., FERRE D., VIGNAUD D., *J. Phys. Colloq. France* **40** (1983) C6-115.
- [20] LANNOO M., The hand book of surfaces and interfaces. Ed. Dobrzynski (New York) vol. 1 (1978) p. 11.
- [21] MERTEN L., *Phys. Kondens. Mater.* **2** (1964) 53.
- [22] LEVINSON I. B., *Sov. Phys. Solid state* **7** (1965) 2336.
- [23] SAADA G., *Phys. Status Solidi (b)* **44** (1971) 717.

- [24] FAIVRE G., SAADA G., *Phys. Status. Solidi (b)* **52**, p. 127.
- [25] VIGNAUD D., FARVACQUE J. L., FERRE D., *Phys. Status Solidi (b)* **110**, p. 601.
- [26] DEXTER D. L., SEITZ F., *Phys. Rev.* **86** (1952) 964.
- [27] BARDEEN J., SHOCKLEY W., *Phys. Rev.* **80** (1950) 72.
- [28] FERRE D., 1987, Thèse d'état (Lille).
- [29] CHOI S. K., MIHARA M., NINOMIYA T. *Jpn J. Appl. Phys.* **16** (1977) 737.
- [30] ASTIE P., COUDERC J. J., CHOMEL P., QUELARD D., DUSEAUX M., *Phys. Status Solidi (a)* **96** (1986) 225.
- [31] FARVACQUE J. L., VIGNAUD D., DEPRAETERE E., SIEBER B., LEFEBVRE A., Proc. 6th Intern. Symposium on structure and properties of dislocations in semiconductors, Oxford 1989 (Inst. Phys. Conf. Ser.).
- [32] VIGNAUD D., 1989, Thèse d'état (Lille).